Terahertz generation by OH1 based on cascaded difference frequency generation

Li Zhongyang, Tan Lian, Bing Pibin, Yuan Sheng

(School of Electric Power, North China University of Water Resources and Electric Power, Zhengzhou 450045, China)

Abstract: Terahertz (THz) wave generation by organic crystal 2 -[3 -(4 -hydroxystyryl) -5,5 -dimethylcyclohex -2 -enylidene]malononitrile (OH1) with a collinear phase-matching scheme based on cascaded difference frequency generation(DFG) processes was theoretically analyzed. The cascaded Stokes interaction processes and the cascaded anti-Stokes interaction processes were investigated from coupled wave equations. THz intensities and quantum conversion efficiency were calculated. Compared with non-cascaded DFG processes, THz intensities from 13 -order cascaded DFG processes were increased to 15.96. The quantum conversion efficiency of 1 377% in cascaded processes can be realized, which exceeds the Manley-Rowe limit.

Key words: terahertz wave; cascaded optical processes; difference frequency generation

CLC number: TN24;O437 **Document code:** A **DOI:** 10.3788/IRLA201645.1025001

OH1 晶体中级联光学差频效应产生太赫兹波

李忠洋,谭 联,邴丕彬,袁 胜

(华北水利水电大学 电力学院,河南 郑州 450045)

摘 要: 理论分析了有机晶体2-[3-(4-hydroxystyryl)-5,5-dimethylcyclohex-2-enylidene]malononitrile(OH1)中基于共线相位匹配级联光学差频产生太赫兹波的物理过程。从耦合波方程出发分析了级联斯托克斯过程和级联反斯托克斯过程,计算了太赫兹波的强度和量子转换效率。相对于非级联光学差频过程,13 阶级联光学差频产生的太赫兹波强度增大了 15.96 倍。13 阶级联光学差频中太赫兹波的量子转换效率为 1377%,超过了 Manley-Rowe 关系的限制。

关键词: 太赫兹波; 级联光学过程; 差频产生

收稿日期:2016-02-14; **修订日期:**2016-03-12

基金项目:国家自然科学基金(61201101,61205003);河南省高等学校青年骨干教师资助计划(2014GGJS-065)

作者简介:李忠洋(1983-),男,副教授,博士,主要从事非线性光学产生太赫兹波方面的研究。Email:thzwave@163.com

0 Introduction

The terahertz (THz) radiation, which is generally referred to as the frequency from 0.1 to 10 THz, has recently drawn much attention due to its tremendous potential applications, such as imaging, material detection, environmental monitoring, communication, astronomy and national defense security[1-4]. For such applications, a high-power, widely tunable, and compact source of THz-wave is required. Due to the interest in exploiting this region, there are many schemes proposed on source technologies over the last twenty years or so [5-10]. Among many electronic and optical methods for the coherent THz -wave generation, difference frequency generation (DFG)[11-14] is of importance because it offers the advantages of relative compactness, narrow linewidth, wide tuning range, high-power output and room-temperature working environment. In DFG, two optical pump beams, with their frequencies separated by a few THz, interact through a $\chi^{(2)}$ process to generate a THz beam. The requirements for nonlinear optical crystal are a high optical nonlinearity and a low absorption coefficient in THz range, more important, allows collinear phase-matching. Organic crystal 4 -*N*, *N* - dimethylamino -4′ -*N*′ -methyl-stilbazolium 2,4,6 - trimethylbenzenesulfonate (OH1) shows a low THz absorption coefficient in the range between 0.3 and 2.5 THz, reaching values lower than 0.2 mm^{-1} between 0.7 and 1.0 THz[15]. Moreover, OH1 has large second-order nonlinear susceptibilities(d_{33}=120 pm/V at 1.9 μm)[16]. THz wave generations from OH1 via collinear phase-matched DFG have been observed[12,17]. Unfortunately, the quantum conversion efficiency is extremely low. To improve the low quantum conversion efficiency and overcome the Manley-Rowe limit, cascaded DFG in which more than one THz photon is generated from the depletion of a single pump photon is a promising method. Theoretical descriptions and experimental demonstrations of an enhancement output of THz wave via cascaded DFG processes have been reported recently[18-20].

In this paper, we present the theoretical analysis of THz generation by OH1 with a collinear phase-matching scheme based on cascaded DFG processes. We investigate the cascaded Stokes interaction processes and the cascaded anti-Stokes interaction processes. THz intensities and quantum conversion efficiency are calculated from coupled wave equations.

1 Theoretical model

Figure 1 shows a schematic diagram of THz wave generation by collinear phase-matching cascaded DFG. THz wave in the OH1 was generated through type-0 phase matching when all the electric fields of pump,

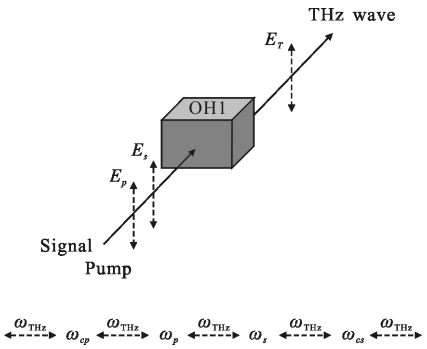

Fig.1 Schematic diagram of the cascaded DFG to generate THz radiation by OH1 crystal

signal and THz waves are parallel to the *c*-axis of the OH1 crystal. THz wave (ω_T) is generated via interactions between the incident pump (ω_p) and signal (ω_s) waves in the first-order DFG process, which consumes the higher frequency pump photon and amplifies the lower frequency signal photon. The amplified signal wave also acts as a higher frequency pump wave, which amplifies the THz wave and generates a new lower frequency cascaded signal (ω_{cs}) wave in the second-order DFG process. Simultaneously, anti-Stokes interactions will also occur that consume the THz photon and pump photon, resulting in a higher frequency anti-Stokes signal (ω_{cp}) wave. The cascaded Stokes processes and anti-Stokes processes

can be continued to any high order as long as the phase-matching conditions are satisfied. The intensity of THz wave is determined by a trade-off between the Stokes processes and the anti-Stokes processes.

The coupled wave equations of cascaded DFG can be derived from common nonlinear optical three-wave interaction equations, shown as:

$$\frac{dE_T}{dz}=-\frac{\alpha_T}{2}E_T+\kappa_T\sum_1^{\infty}E_nE_{n+1}\cos(\Delta k_nz) \quad (1)$$

$$\frac{dE_n}{dz}=-\frac{\alpha_n}{2}E_n+\kappa_nE_{n-1}E_T\cos(\Delta k_{n-1}z)-\kappa_nE_{n+1}E_T\cos(\Delta k_nz) \quad (2)$$

$$\kappa_n=\frac{\omega_n d_{\text{eff}}}{cn_n} \quad (3)$$

$$\Delta k_n=k_n-k_{n+1}-k_T \quad (4)$$

$$\omega_T=\omega_n-\omega_{n-1} \quad (5)$$

$$I=\frac{1}{2}nc\varepsilon_0|E|^2 \quad (6)$$

where ω_n and ω_T denote the frequency of pump and THz wave, respectively. E_n and E_T denote the electric field amplitude of pump and THz wave, respectively. α_n and α_T denote the absorption coefficient of pump and THz wave in the optical crystal, respectively. Δk_n indicates the wave vector mismatch in the cascaded DFG process, κ_n is the coupling coefficient, d_{eff} is the effective nonlinear coefficient, c is the speed of light in vacuum, ε_0 is the vacuum dielectric constant, I is the power density, n_n is the refractive index. The theoretical values of refractive index are calculated using a wavelength-independent Sellmeier equation for OH1 in the IR[16] and THz[15] range, respectively.

2 Calculations

Here, in simulating the cascaded DFG dynamics, pump wave ω_p and signal wave ω_s are supposed to be 217 THz and 216 THz, respectively. THz frequency ω_T is taken to be 1.0 THz. The wave vector mismatch Δk and coherence length in cascaded DFG processes is shown in Fig.2. In the cascaded Stokes processes, wave vector mismatch is less than 3.14 cm^{-1} during a 7-order cascaded processes. In the case of cascaded anti-Stokes processes, wave vector mismatch is less than 3.14 cm^{-1} during a 6-order cascaded processes. In the following calculations, 7-order cascaded Stokes processes and 6-order cascaded anti-Stokes processes are taken into account as the coherence length is larger than 1 cm. As shown in Fig.3, THz intensities based on cascaded Stokes processes and anti-Stokes processes with cascading orders 1, 4, 7, 10 and 13 versus crystal length are calculated according to Eqs. (1) and (2). Pump wave ω_p and signal wave ω_s are supposed to be 223 and 222 THz, respectively. Both of the intensity of pump and signal wave are 20 MW/mm^2. The nonlinear coefficient of OH1 crystal is 120 pm/V at pump frequencies[16], and the absorption coefficients at 1.0 THz is 2.1 cm^{-1}[15]. From the Fig.3 we find that

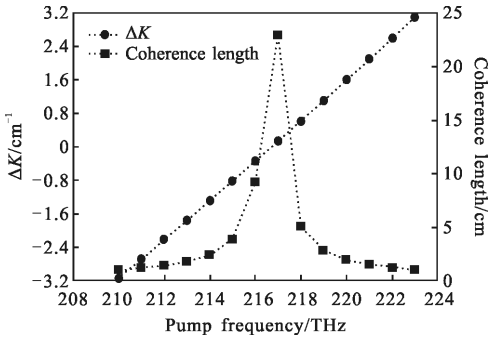

Fig.2 Wave vector mismatch and coherence length of cascaded DFG

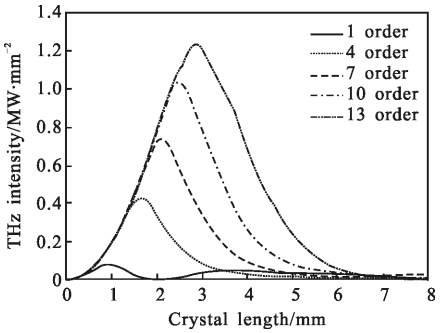

Fig.3 THz intensities by OH1 based on cascaded DFG with cascading orders 1, 4, 7, 10 and 13

THz intensities without cascading processes are extremely low. THz intensities with cascading order 4, 7, 10 and 13 are enhanced. THz intensity of 1.235 MW/mm^2 can be obtained with 13-order cascaded stokes processes. Compared with non-cascaded DFG processes, THz intensities from 13-order cascaded DFG processes are

increased to 15.96. In a non-cascaded DFG processes, at best, a single THz photon is generated from each pump photon. The cascaded processes can enhance the THz output, simply by generating several THz photons from each pump photon.

As the Stokes processes generate THz photon and the anti-Stokes processes consume THz photon, THz intensities depend on the Stokes processes and the anti-Stokes processes. Figure 4 shows the maximum intensities of the optical waves during the cascaded Stokes processes and anti-Stokes processes. In this figure we assume that the optical waves at interval of 1.0 THz with frequencies from 211 THz to 223 THz interact in the Stokes and anti-Stokes processes. The initial pump and signal waves are 217 THz and 216 THz with a power density of 20 MW/mm^2, respectively. From the figure we find that the power densities of optical waves in the Stokes processes is higher than that of optical waves in the anti-Stokes processes, which indicates that the Stokes processes is stronger than the anti-Stokes processes.

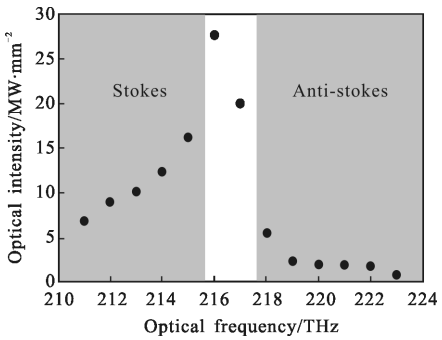

Fig.4 Maximum intensity of the optical waves during the cascaded Stokes processes and anti-Stokes processes

Figure 5 shows the relationship between the maximum THz intensities and pump wave frequencies. In this figure we assume that the optical waves at interval of 1.0 THz with frequencies from 213 THz to 222 THz interact in the cascaded Stokes and anti-Stokes processes. The frequency of pump wave is 1.0 THz larger than that of the signal wave. Both of the pump and signal intensity are 20 MW/mm^2. From the figure we find that THz intensities are higher as the pump frequencies locate in the high-frequency area. The higher THz intensities originate from the interaction of the high-order Stokes processes as the pump frequencies locate in the high-frequency area, which indicates that the Stokes processes is stronger than the anti-Stokes processes. As the pump frequency equals to 222 THz, THz wave with a maximum intensity of 1.034 MW/mm^2 can be obtained. In the high-frequency area where high-order Stokes processes interact, optimal crystal lengths are longer considering cascading, which is consistent with the principle of cascaded nonlinear processes.

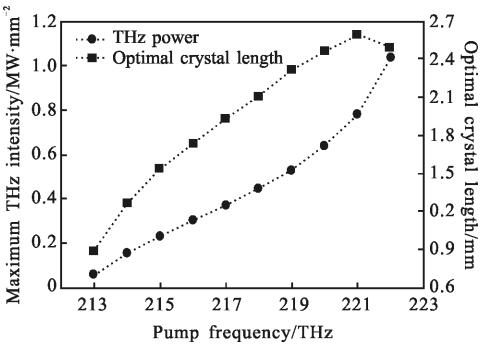

Fig.5 Relationship between the maximum THz intensities and pump frequencies

Pump intensity is directly related to the quantum conversion efficiency in a cascaded DFG processes. The maximum THz intensity and quantum conversion efficiency are calculated when the original pump intensities are changed from 0 MW/mm^2 to 20 MW/mm^2, as shown in Fig.6. In the calculations, pump wave

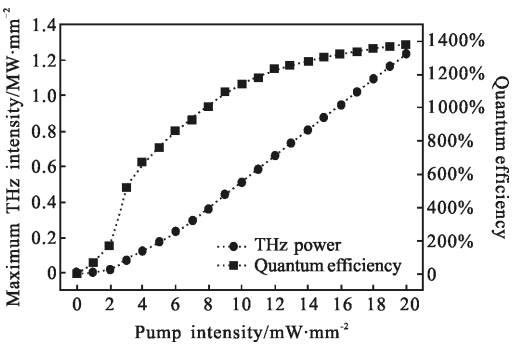

Fig.6 Maximum THz intensity and quantum conversion efficiency versus pump intensity

and signal wave are supposed to be 223 and 222 THz, respectively. Figure 6 demonstrates that the maximum THz intensity and quantum conversion efficiency significantly increases with the pump intensity. THz wave with a maximum intensity of 1.235 MW/mm^2 can be generated as pump intensity equals to 20MW/mm^2, corresponding to the quantum conversion efficiency of 1 377%. The quantum conversion efficiency of 1 377% in cascaded processes exceeds the Manley-Rowe limit.

3 Conclusion

THz generation by organic crystal OH1 with a collinear phase-matching scheme based on cascaded difference frequency generation (DFG) processes is theoretically analyzed. The cascaded DFG processes comprise the Stokes interaction processes and the cascaded anti-Stokes interaction processes. The calculation results indicate that the Stokes processes is stronger than the anti-Stokes processes. Compared with non-cascaded DFG processes, THz intensities from 13-order cascaded DFG processes are increased to 15.96 THz wave with a maximum intensity of 1.235 MW/mm^2 can be generated as pump intensity is 20 MW/mm^2, corresponding to the quantum conversion efficiency of 1 377%. The quantum conversion efficiency of 1 377% exceeds the Manley-Rowe limit, which provide us an efficient way to enhance the output of THz wave.

References:

[1] Su J P, Ma F Y, Yu Z F, et al. Theoretical design of terahertz-wave parametric oscillator based on $LiNbO_3$ crystal [J]. ***Infrared and Laser Engineering***, 2010, 39(3): 482-486. (in Chinese)

[2] Lu Y M, Wang J C, Shi J M, et al. Application of THz technology for detection in soot and wind-blown sand [J]. ***Infrared and Laser Engineering***, 2010, 39(3): 487-490. (in Chinese)

[3] Johnston M. Plasmonics: Superfocusing of terahertz waves [J]. ***Nature Photon***, 2007, 1: 14-15.

[4] Tonouchi M. Cutting-edge terahertz technology [J]. ***Nature Photon***, 2007, 1: 97-105.

[5] Köhler R, Tredicucci A, Beltram F, et al. Terahertz semiconductor-heterostructure laser [J]. ***Nature***, 2002, 417: 156-159.

[6] Yeh K L, Hoffmann M C, Hebling J, et al. Generation of 10 μJ ultrashort terahertz pulses by optical rectification [J]. ***Appl Phys Lett***, 2007, 90(17): 171121.

[7] Williams B S. Terahertz quantum-cascade lasers [J]. ***Nature Photon***, 2007, 1: 517-525.

[8] Carr G L, Martin M C, McKinney W R, et al. High-power terahertz radiation from relativistic electrons [J]. ***Nature***, 2002, 420: 153-156.

[9] Ding Y J. Quasi-single-cycle terahertz pulses based on broadband-phase-matched difference-frequency generation in second-order nonlinear medium: high output powers and conversion efficiencies [J]. ***IEEE J Sel Top Quantum Electron***, 2004, 10(5): 1171-1179.

[10] Knap W, Lusakowski J, Parenty T, et al. Terahertz emission by plasma waves in 60 nm gate high electron mobility transistors [J]. ***Appl Phys Lett***, 2004, 84(13): 2331-2333.

[11] Ding Y J. Progress in terahertz sources based on difference-frequency generation [Invited][J]. ***J Opt Soc Am B***, 2014, 31(11): 2696-2711.

[12] Majkic A, Zgonik M, Petelin A, et al. Terahertz source at 9.4 THz based on a dual-wavelength infrared laser and quasi-phase matching in organic crystals OH1 [J]. ***Appl Phys Lett***, 2014, 105(14): 141115.

[13] Dolasinski B, Powers P E, Haus J W, et al. Tunable narrow band difference frequency THz wave generation in DAST via dual seed PPLN OPG [J]. ***Opt Express***, 2015, 23(3): 3669-3680.

[14] Saito K, Tanabe T, Oyama Y. Design of a GaP/Si composite waveguide for CW terahertz wave generation via difference frequency mixing [J]. ***Appl Opt***, 2014, 53(17): 3587-3592.

[15] Brunner F D J, Kwon O P, Kwon S J, et al. A hydrogen-bonded organic nonlinear optical crystal for high-efficiency terahertz generation and detection [J]. ***Opt Express***, 2008, 16 (21): 16496-16508.

[16] Hunziker C, Kwon S J, Figi H, et al. Configurationally locked, phenolic polyene organic crystal 2 -{3 -(4 -hydroxystyryl) -5,5 -dimethylcyclohex -2 -enylidene} malononitrile: linear and nonlinear optical properties [J]. ***J Opt Soc Am B***, 2008, 25(10): 1678-1683.

[17] Uchida H, Sugiyama T, Suizu K, et al. Generation of widely

tunable terahertz waves by difference-frequency generation using a configurationally locked polyene 2-[3-(4-hydroxystyryl)-5, 5-dimethylcyclohex-2-enylidene] malononitrile crystal [J]. ***Terahertz Sci Technol***, 2011, 4(3): 132-136.

[18] Liu P, Xu D, Yu H, et al. Coupled-mode theory for Cherenkov-type guided-wave terahertz generation via cascaded difference frequency generation [J]. ***J Lightwave Technol***, 2013, 31(15): 2508-2514.

[19] Lee A J, Pask H M. Cascaded stimulated polariton scattering in a Mg:LiNbO3 terahertz laser [J]. ***Opt Express***, 2015, 23 (7): 8687-8698.

[20] Saito K, Tanabe T, Oyama Y. Cascaded terahertz-wave generation efficiency in excess of the Manley-Rowe limit using a cavity phase-matched optical parametric oscillator [J]. ***J Opt Soc Am B***, 2015, 32(4): 617-621.